Authors' response to review of "Northern high-latitude permafrost and terrestrial carbon response to solar geoengineering" by Chen et al.

We thank your constructive comments, which help us clarify and greatly improve the study. In the following, comments from the referee are in black, our responses are in blue.

The authors used a suit of models to explore the potential impact of solar engineering on permafrost carbon dynamics. They mainly found that the permafrost carbon feedback will be greatly inhibited in the scenario of solar engineering, and the permafrost ecosystems remains a carbon sink and the solar engineering will delay the transition of ecosystem carbon cycle from sink to source.

First, the historical simulations have a large deviation from the observed permafrost in terms of area and active layer thickness. The model evaluation needs to be performed in a great detail. Such model deficiency could definitely introduce significant biases into our understanding of the solar engineering impact on the permafrost dynamics. Whether these biases would undermine the main results and conclusions are yet to be determined. The authors should explore the model biases and their potential sources, and discuss the potential impact of these biases on the results. Such model biases would also be present in the simulated terrestrial carbon components such as NPP and ecosystem respiration.

Thanks for your comments. We have taken great care to analyze the model results, and have added a completely new group of land-only experiments to examine the response of northern high-latitude permafrost and terrestrial carbon and compare it with outputs from the full-coupled earth system models (ESMs).

The simulated historical permafrost areas, defined by the annual maximum active layer thicknesses (ALT) ≤3 m, are considerably underestimated in three ESMs (IPSL-CM6A-LR, MPI-ESM1-2-LR and UKESM1-0-LL). The deviation from the observed permafrost status can be ascribed mainly to the biases in the simulated near-surface air temperature and thermal offsets of snow and surface soil layers. UKSEM1-0-LL tends to underestimate summer near-surface air temperature (Figure R1a), but its soil depth is too shallow (the node depth of bottom layer is less than 3 m) to simulate properly soil temperatures in northern high-latitude. Additionally, its recently added multilayered snow scheme produces a too large snow thermal insulation in winter (Figure R1b), the combined effects lead to a large increase in the mean annual ground temperature (MAGT) and much less permafrost, which has been analyzed in a previous study by Burke et al., (2020). IPSL-CM6A-LR and MPI-ESM1-2-LR show relatively smaller deviation in near-surface air temperature, and they have sufficiently deep soil profiles. But the ground thaws too quickly in the summer, likely because the two models do not consider the latent heat of water-phase change (Burke et al., 2020) and consequently lead to much smaller thermal insulation of top surface layer in summer (Figure R1c). More reasonable representation of northern high-latitude snow and soil processes should be considered in these models in future developments.

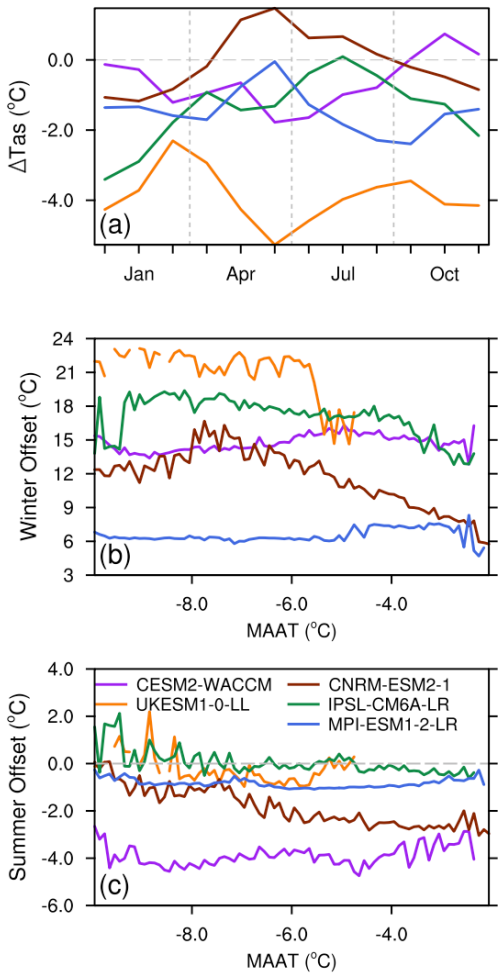

Figure R1. Climatological monthly near-surface air temperature biases and thermal offsets of each ESM. Panel (a) shows the biases in the simulated temperature compared with the observation dataset from Climatic Research Unit gridded Time Series Version 4 (CRU Ts v4, Harris et al., 2020). Panel (b) and (c) show the median values of thermal offsets vs mean annual air temperature (MAAT) in winter and summer. The thermal offset is calculated as the differences between soil temperature at 0.2 m depth and near-surface air temperature. Only grid cells where the winter mean near-surface air temperatures are between -25 and -15 ºC during the baseline period 1995-2014 are shown.

The large deviation in the simulated permafrost area, ALT and soil carbon storage can mislead our understanding of the solar engineering impacts on the permafrost dynamics. The uncertainties in high-latitude permafrost region derived directly from ESMs' results could be separated into two parts: ESMs' responses to future climate scenarios, and inter-model differences in representing land surface processes. To disentangle the impacts due to uncertainties of the ESMs' response to future climate scenarios, we use the anomaly forcing method to drive the latest Community Land Model version 5 (CLM5) with near-surface climate change signals derived from each ESM's future scenario simulations. The anomaly forcing method can effectively capture the relative changes between scenarios in terms of near-surface climate fields required to drive an offline land model. This method has been used by the Permafrost Carbon Network model intercomparison project (McGuire et al., 2018). Comparing the results of the anomaly forcing CLM5 simulations and the

ESMs simulations is helpful to understand the main sources of the uncertainties in the simulated northern high-latitude permafrost and terrestrial carbon response under solar geoengineering scenarios.

The CLM5 is a state-of-the-art land surface model that includes substantial processes associated with permafrost simulation, such as canopy snow processes, cryoturbation, decomposition limitation for frozen soils, vertically resolved soil carbon content (Lawrence et al., 2018). CLM5 can reasonably reproduce historical permafrost extent and soil carbon storage in northern high-latitude permafrost region (Lawrence et al., 2019). CLM5 offers a built-in function supporting the anomaly forcing method by applying precalculated future monthly anomaly signals to user-defined historical sub-daily reference forcing data (Lawrence et al., 2015). In our newly added experiments, monthly anomaly forcing datasets are created for each ESM's four future climate scenarios (G6solar, G6sulfur, ssp245 and ssp585) against their corresponding historical simulation during the period 2005-2014, including temperature, radiation, precipitation, pressure, wind, and specific humidity. CLM5 reconstructs new sub-daily forcing data by applying these precalculated monthly anomaly forcing on top of the 3-houly Global Soil Wetness Project forcing dataset (GSWP3, http://hydro.iis.u-tokyo.ac.jp/GSWP3/), which is also used to drive CLM5 for its spin-up and historical simulation from 1850 to 2014 in this study.

In the CLM5 historical simulation driven by GSWP3 forcing dataset, the simulated permafrost area is 12.6 million km^2 in the baseline period (1995-2014), which is comparable to 12.21-16.98 million km^2 from observation (Zhang et al., 2000), 15.1±2.8 million km^2 from statistical modelling (Aalto et al., 2018), 13.9 million km^2 from equilibrium state modeling of temperature at the top of permafrost (Obu et al., 2019), and 12.3 million km^2 derived from the observation based MAAT-permafrost probability relationship in the manuscript. The simulated soil carbon stock in the northern high-latitude permafrost region is 1137 PgC, a reasonable amount compared to the observation of 1035 PgC in the top 3 m soil (Hugelius et al., 2014).

Table R1 shows changes in NPP, Rh, NEP, vegetation carbon, soil carbon and terrestrial carbon stocks during the period 2080-2099 relative to the baseline period 1995-2014 in both the anomaly forcing CLM5 simulations and the ESMs simulations. During the baseline period in the permafrost region, both CLM5 and ESMs simulate a slightly larger NPP (2.9 PgC yr^{-1} in CLM5, 2.7±0.7 PgC yr^{-1} in ESMs) than Rh (2.7 PgC yr^{-1} in CLM5, 2.5±0.6 PgC yr^{-1} in ESMs). The more rapid growth in Rh than NPP in the anomaly forcing CLM5 simulations leads to decreases in NEP. In contrast, the ESMs simulated growth in Rh is slower than NPP, and NEP increases. By the end of this century, the soil carbon storage in the northern high-latitude permafrost region decreases in the anomaly forcing CLM5 simulations, while it increases in the ESM simulations.

Table R1. Changes in NPP, Rh NEP, vegetation carbon, soil carbon, terrestrial carbon over the baseline permafrost region during the period 2080-2099 relative to baseline period 1995-2014 for the anomaly forcing CLM5 simulations and the ESM simulations.

		G6solar	**G6sulfur**	**ssp245**	**ssp585**
NPP (Pg C yr^{-1})	CLM5	2.1±0.3	2.0±0.5	1.7±0.2	2.9±0.3
	ESMs	2.0±1.0	1.9±1.0	1.5±0.4	2.5±0.8
Rh (Pg C yr^{-1})	CLM5	2.5±0.5	2.5±0.6	2.0±0.4	3.9±0.5
	ESMs	1.6±0.6	1.6±0.7	1.4±0.4	2.3±0.6

NEP (Pg C yr^{-1})	CLM5	-0.5±0.2	-0.7±0.2	-0.5±0.2	-1.2±0.3
	ESMs	0.3±0.4	0.2±0.4	0.1±0.1	0.2±0.4
Vegetation C (Pg C)	CLM5	11.7±1.0	11.6±1.4	9.7±0.8	14.5±1.0
	ESMs	15.7±2.6	15.2±2.4	13.5±2.0	18.7±2.8
Soil C (Pg C)	CLM5	-15.4±7.2	-19.8±7.5	-14.9±7.2	-32.3±9.2
	ESMs	17.7±8.0	16.4±7.5	13.6±5.7	13.0±8.0
Terrestrial C (Pg C)	CLM5	-3.5±6.8	-8.3±6.6	-4.9±6.7	-18.3±8.7
	ESMs	32.2±10.0	30.6±9.5	26.1±6.8	30.8±9.6

The across-model spreads of NPP in the anomaly forcing CLM5 simulations are about half of that in the ESMs simulations (Figure R2a), indicating the differences in near-surface climate fields and the differences in land surface processes represented by the ESMs exert similar impacts on the NPP changes. The spread of Rh changes is of similar magnitude for the anomaly forcing CLM5 simulations and the ESMs simulations (Figure R2b), implying that differences in land surface processes produce much smaller impacts than differences in near-surface climate fields. However, the accumulated impacts of carbon fluxes due to differences in the ESMs' land surface processes lead to much profound impacts on terrestrial carbon pools as evidenced by much larger uncertainties in the ESMs simulations than in the anomaly forcing CLM5 simulations (Figure R2d-f). On the other hand, the differences in land surface processes do affect the magnitudes of soil carbon storage in the permafrost region and its decomposition rates (Walz et al., 2017), which then determines whether the soil carbon storage increases or decreases under future climate scenarios.

As CLM5 simulates a realistic soil carbon storage in northern high-latitude permafrost region, it is expected that more soil carbon in the permafrost region to be exposed under unfrozen conditions in the anomaly forcing CLM5 simulations than in the ESMs simulations. The simulated Rh in the northern permafrost region shows much greater increases than the southern region (Figure R3), leading to negative NEP (Figure R2c) and losses in soil carbon storage and terrestrial carbon storage in all four scenarios, which are opposite to the results from the ESMs simulations (Figure R2e-f). However, in both the anomaly forcing CLM5 simulations and the ESMs simulations, soil carbon storages are higher under G6solar and G6sulfur than ssp585. Thereafter, our conclusion that soil carbon would increase under G6solar and G6sulfur relative to ssp585 is robust although there are large differences in the ESMs' land surface processes.

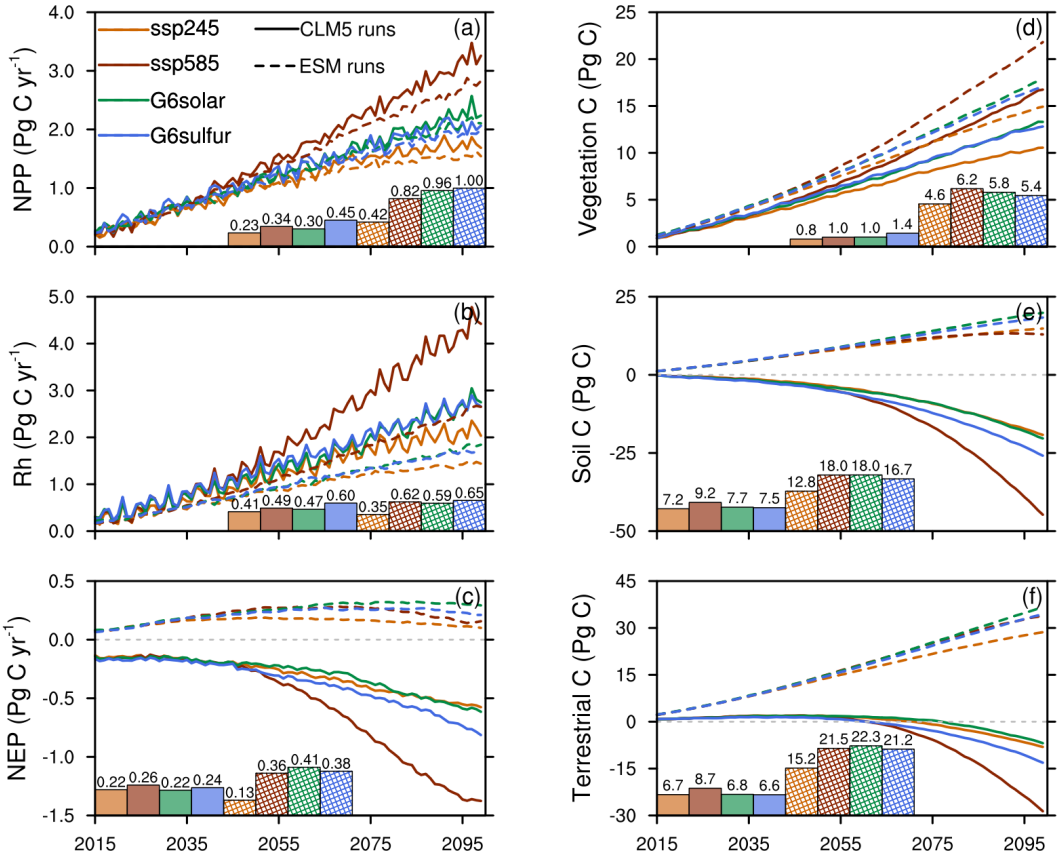

Figure R2. The multi-model ensemble mean of terrestrial carbon fluxes and carbon storage changes over the baseline permafrost region. The left column shows changes in NPP (a), Rh (b) and NEP (c) relative to the baseline period 1995-2014 under ssp245, ssp585, G6solar and G6sulfur. The right column shows changes in vegetation (d), soil (e) and terrestrial (f) carbon storages relative to the baseline period 1995-2014 under ssp245, ssp585, G6solar and G6sulfur. In each panel, bar charts denote one standard derivation from the multi-model ensemble mean averaged over the period 2080-2099, and the number above each bar denotes its magnitude. Dashed lines and hatched bars represent the anomaly forcing CLM5 simulations. Solid lines and solid filled bars represent the ESMs simulations. In panel (c), an 11-year running average is applied on NEP time series to filter its large inter-annual variation.

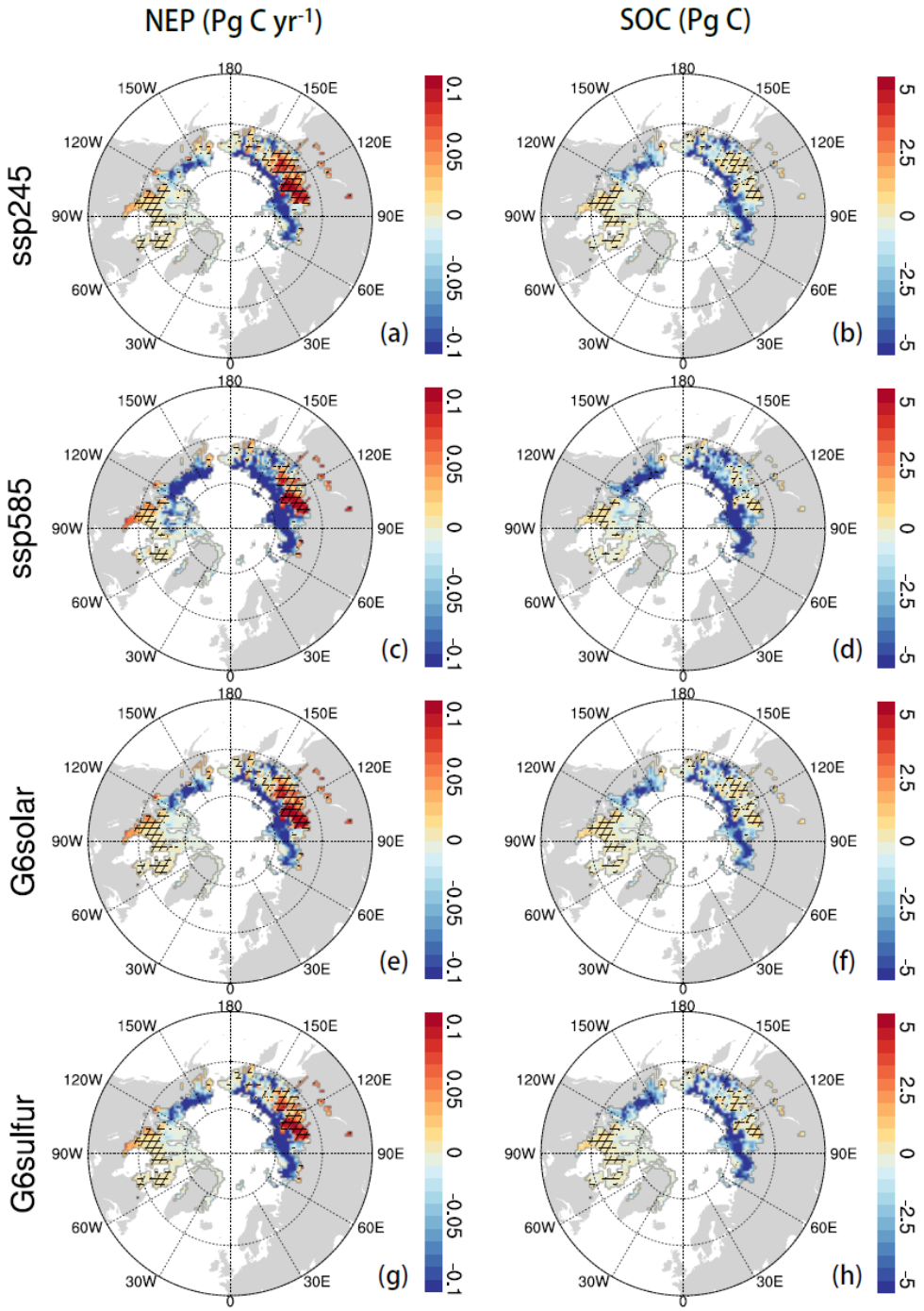

Figure R3. The multi-model ensemble mean changes in NEP (a, c, e, g) and soil carbon storage (b, d, f, h) averaged for the period 2080-2099 relative to the baseline period 1995-2014 under ssp245, ssp585, G6solar and G6sulfur over the baseline permafrost region. Hatched area indicates where the sign of change is same for the anomaly forcing CLM5 simulations and corresponding ESM simulations in terms of multi-model ensemble mean changes.

Second, I strongly disagree with the use of permafrost carbon throughout the manuscript. Almost all of the models did not really consider the permafrost carbon processes (freezing impact on decomposition, cryoturbation etc). Moreover, the models could even fail to capture the magnitude of permafrost carbon storage. The use of observation soil carbon data in this study did not consider the yedoma carbon pool, and the results presented here would therefore definitely

mislead the readers. All of the expression related to permafrost carbon should be removed, since this is nothing to do with the real permafrost carbon dynamic processes.

Thanks for your constructive comments. In the five ESMs used in our study, only the land component (CLM5) of CESM2-WACCM considers relatively sophisticated permafrost physical and carbon processes as noted in our reply above. Others models do fail to capture the magnitude of soil carbon storage in the northern permafrost region. This is the very reason that we have carried out new experiments by using the anomaly forcing CLM5 to capture the uncertainties due to this problem.

On the centennial time scale, the soil carbon in the top 3 m depth is the most vulnerable to microbial decomposition and it controls changes in permafrost soil organic carbon stocks. The deeper yedoma contains about 10% of soil carbon in the present permafrost region and approximately 32 Pg C of it is stored in the upper 3 m soil (Strauss et al., 2017). The yedoma carbon pool has not been represented in most of the complex ESMs yet, and more in situ research might be required to better understand its physical processes, evolution and potential impacts. We encourage more modeling communities to engage in the development of yedoma carbon parameterization into ESMs. To avoid misleading readers, we will revise the expression of "permafrost carbon" to "soil carbon in the permafrost region" and "permafrost carbon feedback" to "permafrost carbon-climate feedback" as suggested in Comyn-Platt et al. (2018), McGuire et al. (2018) and Lee et al. (2019). Thank you for pointing out this aspect.

References:

Aalto, J., Karjalainen, O., Hjort, J., and Luoto, M.: Statistical Forecasting of Current and Future Circum-Arctic Ground Temperatures and Active Layer Thickness, Geophys. Res. Lett., 45, 4889-4898, https://doi.org/10.1029/2018GL078007, 2018.

Burke, E. J., Zhang, Y., and Krinner, G.: Evaluating permafrost physics in the Coupled Model Intercomparison Project 6 (CMIP6) models and their sensitivity to climate change, The Cryosphere, 14, 3155-3174, https://doi.org/10.5194/tc-14-3155-2020, 2020.

CLM5 Documentation, https://www.cesm.ucar.edu/models/cesm2/land/CLM50_Tech_Note.pdf, last access: 30 October 2022.

Comyn-Platt, E., Hayman, G., Huntingford, C., Chadburn, S. E., Burke, E. J., Harper, A. B., Collins, W. J., Webber, C. P., Powell, T., Cox, P. M., Gedney, N., and Sitch, S.: Carbon budgets for 1.5 and 2 ºC targets lowered by natural wetland and permafrost feedbacks, Nat. Geosci., 11, 568-573, https://doi.org/10.1038/s41561-018-0174-9, 2018.

Global Soil Wetness Project Phase 3 (GSWP3): http://hydro.iis.u-tokyo.ac.jp/GSWP3/, last access: 30 October 2022.

Harris, I., Osborn, T. J., Jones, P., and Lister, D.: Version 4 of the CRU TS monthly high-resolution gridded multivariate climate dataset, Scientific Data, 7, 109, https://doi.org/10.1038/s41597-020-0453-3, 2020.

Hugelius, G., Strauss, J., Zubrzycki, S., Harden, J. W., Schuur, E. A. G., Ping, C. L., Schirrmeister, L., Grosse, G., Michaelson, G. J., Koven, C. D., O'Donnell, J. A., Elberling, B., Mishra, U., Camill, P., Yu, Z., Palmtag, J., and Kuhry, P.: Estimated stocks of circumpolar permafrost carbon with quantified uncertainty ranges and identified data gaps, Biogeosciences, 11, 6573-6593, https://doi.org/10.5194/bg-11-6573-2014, 2014.

Lawrence, D. M., Koven, C. D., Swenson, S. C., Riley, W. J., and Slater, A. G.: Permafrost thaw and resulting soil moisture changes regulate projected high-latitude CO_2 and CH_4 emissions, Environ. Res. Lett., 10, 094011, https://doi.org/10.1088/1748-9326/10/9/094011, 2015.

Lawrence, D., Fisher, R., Koven, C. D., Oleson, K., Swenson, S., Vertenstein, M. et al., 2018, Technical Description of version 5.0 of the Community Land Model (CLM), http://www.cesm.ucar.edu/models/cesm2/land/CLM50_Tech_Note.pdf

Lawrence, D. M., Fisher, R. A., Koven, C. D., Oleson, K. W., Swenson, S. C., Bonan, G., Collier, N., Ghimire, B., van Kampenhout, L., Kennedy, D., Kluzek, E., Lawrence, P. J., Li, F., Li, H., Lombardozzi, D., Riley, W. J., Sacks, W. J., Shi, M., Vertenstein, M., Wieder, W. R., Xu, C., Ali, A. A., Badger, A. M., Bisht, G., van den Broeke, M., Brunke, M. A., Burns, S. P., Buzan, J., Clark, M., Craig, A., Dahlin, K., Drewniak, B., Fisher, J. B., Flanner, M., Fox, A. M., Gentine, P., Hoffman, F., Keppel Aleks, G., Knox, R., Kumar, S., Lenaerts, J., Leung, L. R., Lipscomb, W. H., Lu, Y., Pandey, A., Pelletier, J. D., Perket, J., Randerson, J. T., Ricciuto, D. M., Sanderson, B. M., Slater, A., Subin, Z. M., Tang, J., Thomas, R. Q., Val Martin, M., and Zeng, X.: The Community Land Model Version 5: Description of New Features, Benchmarking, and Impact of Forcing Uncertainty, J. Adv. Model. Earth Sy., 11, 4245-4287, https://doi.org/10.1029/2018MS001583, 2019.

Lee, H., Ekici, A., Tjiputra, J., Muri, H., Chadburn, S. E., Lawrence, D. M., and Schwinger, J.: The Response of Permafrost and High‐Latitude Ecosystems Under Large‐Scale Stratospheric Aerosol Injection and Its Termination, Earth's Future, 7, 605-614, https://doi.org/10.1029/2018EF001146, 2019.

McGuire, A. D., Lawrence, D. M., Koven, C., Clein, J. S., Burke, E., Chen, G., Jafarov, E., MacDougall, A. H., Marchenko, S., Nicolsky, D., Peng, S., Rinke, A., Ciais, P., Gouttevin, I., Hayes, D. J., Ji, D., Krinner, G., Moore, J. C., Romanovsky, V., Schädel, C., Schaefer, K., Schuur, E. A. G., and Zhuang, Q.: Dependence of the evolution of carbon dynamics in the northern permafrost region on the trajectory of climate change, Proceedings of the National Academy of Sciences, 115, 3882-3887, https://doi.org/10.1073/pnas.1719903115, 2018.

Obu, J., Westermann, S., Bartsch, A., Berdnikov, N., Christiansen, H. H., Dashtseren, A., Delaloye, R., Elberling, B., Etzelmüller, B., Kholodov, A., Khomutov, A., Kääb, A., Leibman, M. O., Lewkowicz, A. G., Panda, S. K., Romanovsky, V., Way, R. G., Westergaard-Nielsen, A., Wu, T., Yamkhin, J., and Zou, D.: Northern Hemisphere permafrost map based on TTOP modelling for 2000‐2016 at

1 km^2 scale, Earth-Sci. Rev., 193, 299-316, https://doi.org/10.1016/j.earscirev.2019.04.023, 2019.

Strauss, J., Schirrmeister, L., Grosse, G., Fortier, D., Hugelius, G., Knoblauch, C., Romanovsky, V., Schädel, C., Schneider Von Deimling, T., Schuur, E. A. G., Shmelev, D., Ulrich, M., and Veremeeva, A.: Deep Yedoma permafrost: A synthesis of depositional characteristics and carbon vulnerability, Earth-Sci. Rev., 172, 75-86, https://doi.org/10.1016/j.earscirev.2017.07.007, 2017.

Walz, J., Knoblauch, C., Böhme, L., and Pfeiffer, E.: Regulation of soil organic matter decomposition in permafrost-affected Siberian tundra soils - Impact of oxygen availability, freezing and thawing, temperature, and labile organic matter, Soil Biology and Biochemistry, 110, 34-43, https://doi.org/10.1016/j.soilbio.2017.03.001, 2017.

Zhang, T., Heginbottom, J. A., Barry, R. G., and Brown, J.: Further statistics on the distribution of permafrost and ground ice in the Northern Hemisphere, Polar geography (1995), 24, 126-131, https://doi.org/10.1080/10889370009377692, 2000.